

# Development of Fluorescent or Phosphorescent Materials for Non-Dopant Red Organic Light-Emitting Diodes

Chin-Ti Chen<sup>1</sup>

Institute of Chemistry, Academia Sinica, Taipei, Taiwan 11529, R. O. C.

## Abstract

In this paper, a renovated approach in the fabrication of red organic light-emitting diodes (OLEDs) is described. The hard-to-control doping process required for dopant-based red OLEDs can be avoided due to the novel red fluorophores that are not concentration quenching in solid state. Doping is in general a must for phosphorescence OLEDs because of the triplet-triplet annihilation, a common problem for phosphorophore dopants. However, we have recently found that extraordinary red iridium complex showing relatively short emission lifetime render the non-doped phosphorescence red OLED possible.

## 1. Introduction

Numerous fluorescent materials, either as host-emitters or dopants,<sup>[1]</sup> have been known and developed since the Kodak's report on green OLED in 1987 and the dopant-based green and red OLEDs in 1989.<sup>[2,3]</sup> Whereas short wavelength light-emitting blue or green fluorescent materials commonly used as either host-emitter or dopant, red fluorescent materials are less flexible and mostly limited to the dopant usage in the fabrication of red OLEDs. This is due to the nature of red fluorescent materials. Fluorophores emitting long enough wavelength (emission maximum wavelength  $\lambda_{\text{max}} > 610$  nm) are usually polar, such as electron-donor-substituted pyran-containing compounds, or non-polar but extensively  $\pi$ -conjugated, such as polycyclic aromatic hydrocarbon (PAH) or porphyrin-type macrocyclic compounds. Red emitters used in OLEDs include materials that are highly emissive in solution, such as Nile Red, DCM (4-(dicyanomethylene)-2-methyl-6-[4-(dimethylaminostyryl)-4H-pyran]), and those more weakly emissive, such as TPP (5,10,15,20-teraphenylporphyrin) (Figure 1).<sup>[4]</sup> However, all these red fluorophores are prone to aggregation in solid state, due to either attractive dipole-dipole interactions or effective intermolecular  $\pi$ -stacking. Therefore, they are highly susceptible to concentration quenching

and become either weakly emissive or even not emissive at all in solid state (Figure 1).

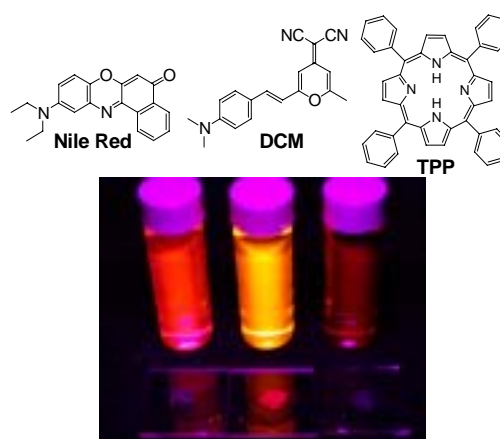


**Figure 1.** Fluorescence image of Nile red (left), DCM (center), and TPP (right) in solution ( $\text{CH}_2\text{Cl}_2$ ) and in solid state. Please note that the fluorescence of the solid samples of Nile red and TPP is virtually invisible (their solid state fluorescence quantum yields are close to nil).

On the other hand, phosphorescent materials, mostly are complexes of heavy transition metals of Ir, Os, and Pt, provide electroluminescence with efficiency three times higher than fluorescent materials. However, triplet-triplet (T-T) annihilation, which is a key adverse factor for the phosphorescence-based emitter, can also be greatly inhibited by dispersing emitter molecules, a doping process. This method has become a standard protocol for the phosphorescent emitters.

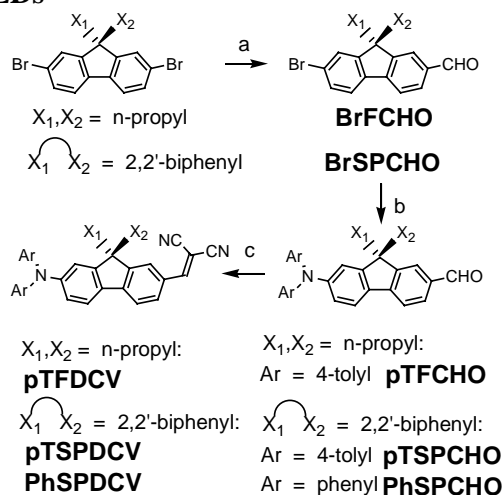
Consequently, guest-host doped emitter system becomes a universal method for solving the problem of these red emissive materials when applied for OLEDs. Dopant molecules are dispersed and isolated in the host materials and thus concentration quenching can be avoided. However, the optimum dopant

<sup>1</sup> cchen@chem.sinica.edu.tw; Fax: +886-2-27831237

concentration is usually low, commonly no greater than 2%, and the effective doping range is extremely narrow and commonly no greater than  $\pm 0.5\%$  of the optimum concentration.<sup>[4]</sup> Realistically, OLEDs based on dopant are more difficult to adapt for mass production process than those based on non-doped host emitter, considering the reproducibility of the optimum doping level requires careful manufacture control. For a practical concern, a solution to the red light-emitting OLEDs, either in materials or devices perspective, is highly needed.

Here, newly developed novel red fluorophores and phosphorophores by our laboratory are illustrated for the usage as rare non-dopant red emitter in the fabrication of red OLED. Their red OLEDs performance are examined and compared with conventional dopant-based red OLEDs.

## 2. Fluorophore-Based Non-Dopant Red OLEDs



**Scheme 1** Reagents and conditions: (a) *n*-BuLi, THF,  $-78\text{ }^\circ\text{C}$ , then DMF, RT, 3 h, 79% (**BrFCHO**), 75% (**BrSPCHO**); (b) di(4-tolyl)amine or diphenylamine,  $\text{Cs}_2\text{CO}_3$ ,  $\text{Pd}(\text{OAc})_2$ ,  $\text{P}(t\text{-Bu})_3$ , toluene,  $120\text{ }^\circ\text{C}$ , 8 h, 86% (**pTFCHO**), 75% (**pTSPCHO**), 95% (**PhSPCHO**); (c) malononitrile, basic  $\text{Al}_2\text{O}_3$ , toluene,  $70\text{ }^\circ\text{C}$ , 16 h, 90% (**pTFDCV**), 76% (**pTSPDCV**), 73% (**PhSPDCV**).

Three newly synthesized non-dopant fluorophores, **pTFDCV**, **pTSPDCV**, and **PhSPDCV** (Scheme 1) are adopted in the fabrication of non-doped red OLEDs.<sup>[5]</sup> However, in solid state, all three fluorene derivatives show red fluorescence with  $\lambda_{\text{max}}^{\text{fl}} > 625$

nm, satisfying the requirement for red OLEDs. In solution (1,4-dioxane), these red fluorophores exhibit intense fluorescence (solution fluorescence quantum yield  $\phi_f$  is 70~75%), comparable with classical red fluorophore Nile Red ( $\phi_f$  is 67%) but much stronger than red laser dye DCM ( $\phi_f$  is 8%). Conversely, they are all much brighter red fluorophores compared with the dull Nile Red or DCM in solid state (see fluorescence images shown in Figure 2).

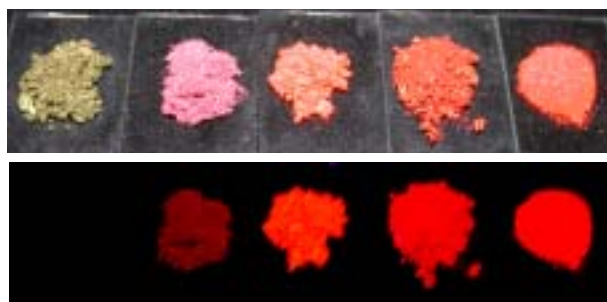


**Figure 2.** White light (top) and UV (bottom) illumination of the powder of Nile Red, DCM, **pTFDCV**, **pTSPDCV**, and **PhSPDCV** (from left to right), respectively.

The measurement of semi-crystalline solid films indicated the solid film fluorescence quantum yields of three red emitting fluorene derivatives are in the range of 25-33%, which are far more higher than ~0% and 5% of Nile Red and DCM, respectively. This should be attributed to the anti-aggregation molecular design (rigid and bulky orthogonal shape of molecules) of the red emitting fluorenes. Therefore, unlike the flat-shape of Nile Red or DCM, **pTFDCV**, **pTSPDCV**, and **PhSPDCV** are all suitable as the red host emitters in the fabrication of non-doped red OLEDs.

**pTFDCV**, **pTSPDCV** and **PhSPDCV** were each adopted in the fabrication of non-doped, red OLEDs of Device I-III with the same configuration for comparison purpose: Device I: ITO/NPB(10 nm)/**pTFDCV** (40nm)/BCP (20nm)/Alq<sub>3</sub>(30 nm)/Mg:Ag; Device II: ITO/NPB(10 nm)/ **pTSPDCV** (40nm)/BCP (20nm)/Alq<sub>3</sub>(30 nm)/Mg:Ag; Device III: ITO/NPB(10 nm)/ **PhSPDCV** (40nm)/BCP (20nm)/Alq<sub>3</sub>(30 nm)/Mg:Ag. Authentic red EL was observed for these devices (Figure 3).

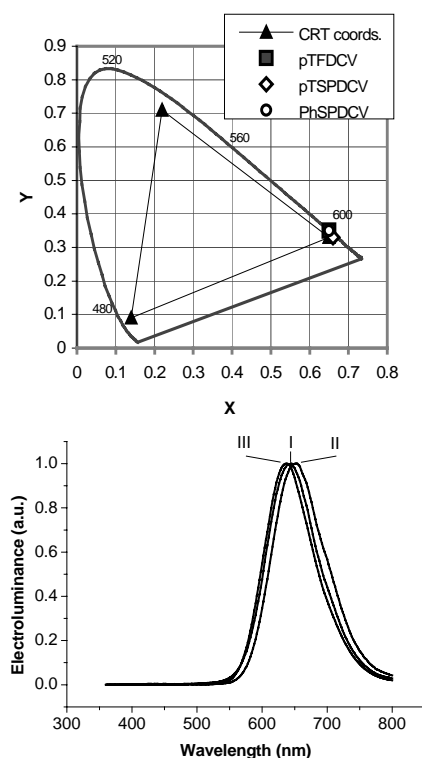


**Figure 3.** CIE 1931 chromaticity diagram (left) and EL spectra (right) of device I, II, and III containing **pTFDCV**, **pTSPDCV**, and **PhSPDCV**, respectively.

They are all sufficiently red and have comparable chromaticity as CRT (Cathode Ray Tube) Phosphors either American or European standard red color according to 1931 CIE (Commission Internationale de l'Eclairage) chromaticity diagram ( $x = 0.63\sim 0.64$ ,  $y = 0.33\sim 0.34$ ).<sup>[6]</sup> Each device can be turned on between 3 and 5 V and showing red EL with the intensity in the range of 300-615  $\text{cd m}^{-2}$  at low current density of 20  $\text{mA cm}^{-2}$  (about 7-8 V), which is sufficient bright and practical for the flat panel display application. Device III shows the highest electroluminescence ( $L$ ) of 11400  $\text{cd m}^{-2}$  and external quantum efficiency ( $\eta_{\text{EXT}}$ ) of 3.6% among the three devices (Figure 4), which is quite consistent with the higher fluorescence quantum yield of **PhSPDCV** than those of **pTFDCV** and **pTSPDCV** in solid state. The performance of fluorene-based non-doped red OLEDs is the best so far<sup>[8]</sup> and comes close to the best of dopant-based red OLEDs (DCJTb as the red dopant having 4.4  $\text{cdA}^{-1}$  maximum efficiency and brightness 966  $\text{cdm}^{-2}$  at 20  $\text{mAcm}^{-2}$ ).<sup>[7]</sup>

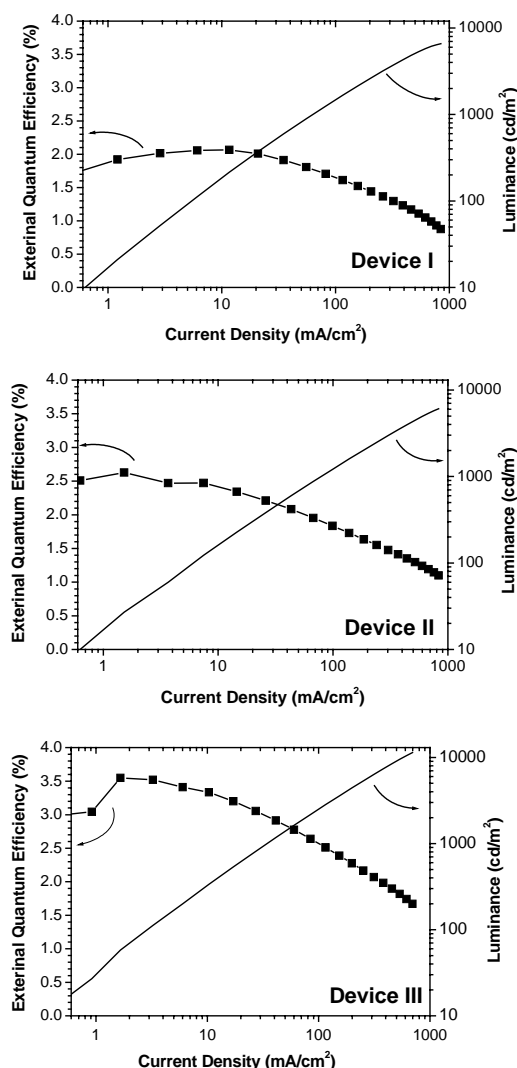
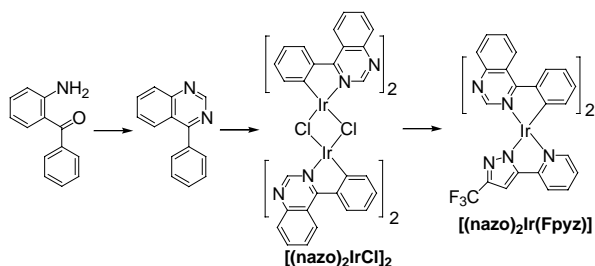


**Figure 4.** EL intensity-external quantum efficiency-current density ( $L$ - $\eta_{\text{EXT}}$ - $I$ ) characteristics of devices I-V.

### 3. Phosphorophore-Based Non-Dopant Red OLEDs

A synthetic pathway leading to the desired Ir complexes is depicted in Scheme 2. First of all, a 4-phenyl substituted quinazoline ligand, (nazo)H, was obtained from a condensation reaction of 2-aminobenzophenone and formamide according to the literature method.<sup>[8]</sup> The subsequent reaction of ligand (nazo)H with  $\text{IrCl}_3 \cdot n\text{H}_2\text{O}$  in refluxing methoxyethanol afforded the chloride bridged dimer

complex  $[(\text{nazo})_2\text{IrCl}]_2$  in a high yield. This dimer complex  $[(\text{nazo})_2\text{IrCl}]_2$  would easily react with the pyridylpyrazole ligand to afford the emissive monomeric complexes with formula  $[(\text{nazo})_2\text{Ir}(\text{Fppz})]$ .



**Scheme 2.** Synthetic method leading to  $[(\text{nazo})_2\text{Ir}(\text{Fppz})]$ .

$[(\text{nazo})_2\text{Ir}(\text{Fppz})]$  was used in the fabrication of red OLED devices (Table 1) as either dopant (devices IV-VI) or non-doped host-emitter (device VII). For Device IV-VI, as they became brighter and more efficient when the doping level of 1 was increasing in the range of 7 ~ 21%. To our knowledge, this is in contrast to most of the literature reports in which an upper limit of the doping level is ~ 10%, except for the case where the pinene group was introduced to suppress the aggregation quenching.<sup>[9]</sup>

**Table 1.** EL characteristics of OLEDs (devices I-VIII)

	Max. EL Intensity [ $\text{cd m}^{-2}$ ] <sup>[b]</sup>	$\phi^{\text{el[c]}}$ [%]	Max. $\phi^{\text{el}}$ [%, $\text{cd A}^{-1}$ , $\text{lm W}^{-1}$ ]	EL $\lambda_{\text{max}}$ [nm]	CIE [x,y]
IV <sup>[a]</sup>	58570 (14010, 3160)	6.8(12), 7.7(10)	8.0, 16.4, 5.9	600	0.59, 0.39
V <sup>[a]</sup>	45200 (12370, 2840)	7.1(12), 8.1(10)	8.1, 14.0, 4.9	606	0.62, 0.37
VI <sup>[a]</sup>	38180 (11990, 2870)	7.3(12), 8.7(10)	8.8, 14.5, 5.0	610	0.63, 0.37
VII <sup>[a]</sup>	29790 (5780, 1330)	5.5(10), 6.3(8)	6.3, 6.7, 2.7	626	0.66, 0.34

[a] Device IV-VII: ITO/NPB(40 nm)/ $[(\text{nazo})_2\text{Ir}(\text{Fppz})]$ :CBP(x%, 30 nm)/BCP (10 nm)/Alq3 (30 nm)/Mg:Ag, x = 7, 14, 21, 100%, respectively. [b] Numbers in parenthesis are the electroluminescence at current density of 100 and 20  $\text{mA cm}^{-2}$ . [c] External quantum efficiency at the current density of 100 and 20  $\text{mA cm}^{-2}$ . Numbers in parenthesis are the corresponding voltage.

The unexpected success at high doping levels prompted us to adopt a non-doped, host-emitting approach in the fabrication of the fourth device (Device VII in Table 1). Whereas devices IV-VI showed unsatisfactory orange-red EL, Device VII clearly showed a deep red EL with  $\lambda_{\text{max}}$  at 626 nm (Figure 5) corresponding to (0.66, 0.34) of 1931 CIE chromaticity (Table 1).

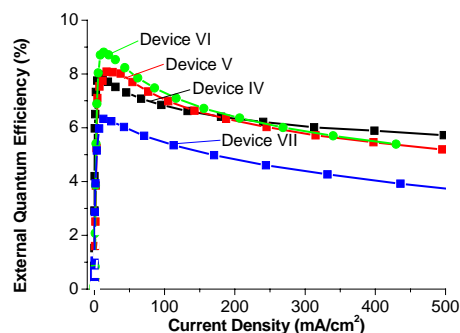
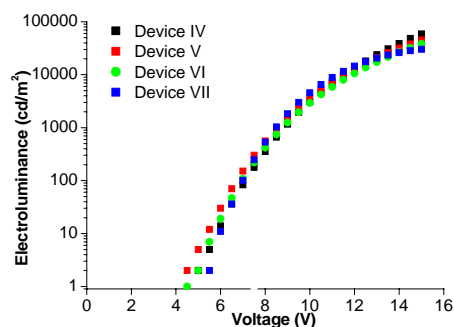
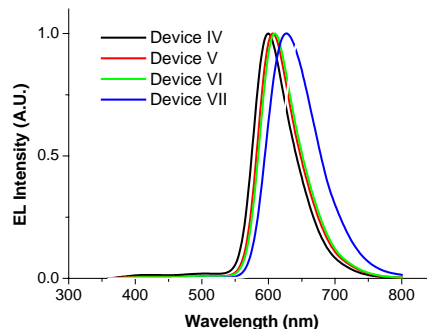


**Figure 5.** EL spectra (top), voltage dependency of electroluminescence (center), and current density dependency of external quantum efficiency (bottom) of OLED devices I, II, III, and IV.

The performance of this authentic red, non-doped OLED is remarkable, considering that the sufficient luminance (1330  $\text{cdm}^{-2}$ ) and the good efficiency (6.3%, 6.7  $\text{cdA}^{-1}$ , or 2.5  $\text{lmW}^{-1}$ ) were successfully

achieved at a practical current density of 20 mAcm<sup>-2</sup>. To the best of our knowledge, the results here successfully demonstrate for the first time a phosphorescence-based red OLED fabricated using a non-doped architecture, and the devices retained sufficiently bright and efficient. Moreover, in comparison with other red OLEDs based on Ir-complex dopant, Device IV-VI suffered moderately from the decay of efficiency at a elevated current density (Figure 4). Particularly, very similar decreasing efficiency along with increasing current density was found for all devices, regardless the dopant concentration of the device, including the non-dopant device (Device VII). Such unusual performance can be all attributed to the relatively short emission lifetime of [(nazo)<sub>2</sub>Ir(Fppz)] (see below).

Complex [(nazo)<sub>2</sub>Ir(Fppz)] exhibits an intensive emission maximized at 607 nm ( $\Phi = 0.52$ ) with a emission lifetime ( $\tau$ ) measured to be as short as 1.05  $\mu$ s in degassed CH<sub>2</sub>Cl<sub>2</sub> (Table 1).

**Table 2.** Photophysical properties of [(nazo)<sub>2</sub>Ir(Fppz)]

$\lambda_{\max}^{\text{abs}}, (\epsilon)$ [nm],[M <sup>-1</sup> cm <sup>-1</sup> ]	PL $\lambda_{\max}^{\text{[a]}}$ [nm]	$\Phi^{\text{[a]}}$ degassed	$\tau^{\text{[a]}}$ [ $\mu$ s]
565, (1330)	607	0.52	1.05
525, (2150)	(634)	(0.41)	(0.40)
470, (3970)			

[a] in CH<sub>2</sub>Cl<sub>2</sub> and data in parenthesis show the property in solid state.

Such short emission lifetime of <1  $\mu$ s is rather unusual and is significantly shorter than those of other known red phosphorescence emitters, such as Pt(OEP) (~50  $\mu$ s),<sup>[10]</sup> Ir(btp)<sub>2</sub>(acac) (4  $\mu$ s),<sup>[10]</sup> and Ir(piq)<sub>2</sub>(acac) (1.7  $\mu$ s),<sup>[11]</sup> and comparable with that of the best performing Ir(tiq)<sub>3</sub> and Ir(fliq)<sub>3</sub> (0.74  $\mu$ s).<sup>[12]</sup> We believe that the short radiative lifetime could be pivotal for rationalizing the strong electrophosphorescence from this simplified device structure. Our finding would be of particular importance for fabricating much simpler and easy-fabrication device architecture. Based on the argument here, this non-doped device architecture should be equally applicable to other phosphorescent emitters, so long as a short radiative lifetime of red

phosphores in the solid state.

#### 4. Acknowledgements

This work is partly supported by National Science Council of Taiwan. The author also thanks for Prof. Yun Chi of National Tsing Hua University and Prof. Pi-Tai Chou of National Taiwan University in preparing sample and photophysical measurement of novel [(nazo)<sub>2</sub>Ir(Fppz)]. Financial support from Academia Sinica and the instruction from Prof. Yu-Tai Tao in device fabrication and measurement are acknowledged as well.

#### 5. References

- [1] Chen, C.H.; Shi, J.; Tang, C.W. *Macromol. Symp.* 125, 1 (1997).
- [2] Tang, C. W. and VanSlyke, S. A. *Appl. Phys. Lett.* 51, 913 (1987).
- [3] Tang, C. W.; VanSlyke, S. A.; Chen, C. H. *Appl. Phys. Lett.*, 65, 3610 (1989).
- [4] Chen, C.-T. *Chem. Mater.* 16, 4389 (2004).
- [5] Chiang, C.-L.; Wu, M.-F.; Dai, D.-C.; Wen, Y.-S.; Wang, J.-K.; Chen, C.-T. *Adv. Funct. Mater.* 15, 231 (2005).
- [6] Copper, A. D.; Cok, R. S.; Feldman, R. D. *SPIE - Int. Soc. Opt. Eng.* 4105, 18 (2001).
- [7] Liu, T. -H.; Iuo, C. -Y.; Chen, C. H. *Appl. Phys. Lett.* 83, 5241 (2003).
- [8] Song, Y.-H.; Yeh, S.-J.; Chen, C.-T.; Chi, Y.; Liu, C.-S.; Yu, J.-K.; Hu, Y.-H.; Chou, P.-T.; Peng, S.-M.; Lee, G.-H. *Adv. Funct. Mater.* 14, 1221 (2004).
- [9] Xie, H. Z.; Liu, M. W.; Wang, O. Y.; Zhang, X. H.; Lee, C. S.; Hung, L. S.; Lee, S. T.; Teng, P. F. Kwong, H. L.; Zheng, H.; Che, C. M. *Adv. Mater.* 13, 1245 (2001).
- [10] Adachi, M.; Baldo, A.; Forrest, S. R.; Lamanky, S.; Thompson, M.; Kwong, R. C. *Appl. Phys. Lett.* 78, 1622 (2001).
- [11] Su, Y. -J.; Huang, H. -L.; Li, C. -L.; Chien, C. -H.; Tao, Y. -T.; Chou, P. -T.; Datta, S.; Liu, R. -S. *Adv. Mater.* 15, 884 (2003).
- [12] Tsuboyama, A.; Iwawaki, H.; Furugori, M.; Mukaide, T.; Kamatani, J.; Igawa, S.; Moriyama, T.; Miura, S.; Takiguchi, T.; Okada, S.; Hoshino, M.; Ueno, K. *J. Am. Chem. Soc.* 125, 12971 (2003).

**Columns on Last Page Should Be Made As Close to Equal Length**